

EVALUATION-AWARE REINFORCEMENT LEARNING

Shripad Vilasrao Deshmukh Will Schwarzer Scott Niekum

University of Massachusetts Amherst
{svdeshmukh, wschwarzer, sniekum}@cs.umass.edu

ABSTRACT

Policy evaluation is often a prerequisite for deploying safety- and performance-critical systems. Existing evaluation approaches frequently suffer from high variance due to limited data and long-horizon tasks, or high bias due to unequal support or inaccurate environmental models. We posit that these challenges arise, in part, from the standard reinforcement learning (RL) paradigm of policy learning without explicit consideration of evaluation. As an alternative, we propose evaluation-aware reinforcement learning (EvA-RL), in which a policy is trained to maximize expected return while simultaneously minimizing expected evaluation error under a given value prediction scheme—in other words, being “easy” to evaluate. We formalize a framework for EvA-RL and design an instantiation that enables accurate policy evaluation, conditioned on a small number of rollouts in an *assessment environment* that can be different than the deployment environment. However, our theoretical analysis and empirical results show that there is often a tradeoff between evaluation accuracy and policy performance when using a fixed value-prediction scheme within EvA-RL. To mitigate this tradeoff, we extend our approach to co-learn an assessment-conditioned state-value predictor alongside the policy. Empirical results across diverse discrete and continuous action domains demonstrate that EvA-RL can substantially reduce evaluation error while maintaining competitive returns. This work lays the foundation for a broad new class of RL methods that treat reliable evaluation as a first-class principle during training.

1 INTRODUCTION

Policy evaluation is often a prerequisite for deploying RL policies in safety- or performance-critical settings such as industrial control (Gao et al., 2014; Zheng et al., 2021), robotics (Andrychowicz et al., 2020; Kalashnikov et al., 2018) and healthcare (Komorowski et al., 2018; Fox et al., 2021). Evaluation settings are often not representative of deployment settings, due to factors such as data availability, data collection costs, and safety constraints. For example, consider a self-driving car that cannot be exhaustively tested in every possible real-world scenario that it will encounter; instead, it may be tested via a combination of limited tests in the real world (perhaps with professional drivers ready to take over), controlled scenarios such as a test course, tests in simulation, or off-policy evaluation via historical data. More generally, compared to the setting that a policy will be deployed in, evaluation data may be collected in a manner that is off-policy, limited in size, has limited support, or uses an inaccurate model of the environment.

Existing evaluation methods struggle to address these challenges: Off-policy policy evaluation (OPE), while unbiased, tends to suffer from unacceptably high variance as the horizon grows (e.g. importance sampling-based methods (Thomas et al., 2015)) or instability associated with the estimation of steady-state distributions (Liu et al., 2018). In either case, OPE assumes that the support of the behavior policy fully covers the support of the evaluation policy (or similarly for the steady-state distributions) and relies on low

divergence between these quantities for efficient evaluation. Evaluation via limited on-policy data provides an unbiased estimate of performance, but is inherently high variance due to the small number of samples. Testing a fixed subset of situations that will be encountered in the deployment setting or using an inaccurate model generally leads to biased estimation.

Our core insight is that these difficulties are caused, in part, by the fact that the current dominant paradigm in AI is to first learn an arbitrary policy and then perform evaluation afterwards, without consideration for that evaluation at train-time. By contrast, **we propose evaluation-aware policy learning that is explicitly designed to learn policies that can be evaluated efficiently and accurately**. We call this evaluation-aware reinforcement learning (**EvA-RL**).

As our main contribution, we introduce a policy learning framework that steers training towards policies that maximize performance while minimizing evaluation error under a given value-prediction scheme, based on rollouts from an *assessment environment*. This assessment environment is a proxy for the deployment environment—for example, a subset of the deployment environment or a related environment such as a simulation—in which value-informative behavior can be observed more easily, cheaply, or safely than in the deployment environment. Further, we introduce a practical instantiation of this framework for accurate, low-shot policy evaluation. Specifically, an EvA-RL policy gradient learning rule is introduced that considers state-value predictions during training to learn policies with low evaluation error, while also maximizing performance.

A theoretical analysis of this framework reveals a tradeoff between maximizing policy performance and minimizing evaluation error when using a fixed value prediction scheme. We mitigate this tradeoff by co-learning a transformer-based (Vaswani et al., 2017) state-value predictor alongside the policy. This shifts part of the burden of evaluation error minimization onto the predictor itself, easing the constraints on policy learning. Our empirical studies across diverse discrete and continuous control domains demonstrate that EvA-RL consistently reduces evaluation error while maintaining competitive returns.

Taken together, this work opens a new line of research that elevates evaluation to a first-class principle in reinforcement learning, enabling the development of policies that are both performant and supportive of efficient, accurate evaluation.

2 BACKGROUND AND RELATED WORK

Markov Decision Process (MDP). A Markov Decision Process (MDP) (Puterman, 1990) is defined by the tuple $\{\mathcal{S}, \mathcal{A}, P, R, \gamma, \mu\}$, where \mathcal{S} is the state space, \mathcal{A} is the action space, P is the transition probability function, R is the reward function, γ is the discount factor, and μ is the start-state distribution. A policy π specifies a distribution over actions given a state, $\pi : \mathcal{S} \rightarrow \Delta(\mathcal{A})$. We consider a finite-horizon setting, where a trajectory is $h := (s_0, a_0, r_0, \dots, s_{T-1}, a_{T-1}, r_{T-1}, s_T)$ and its return is $g(h) := \sum_{t=0}^{T-1} \gamma^t r_t$. The state-value function of a policy π is $V_\pi(s) := \mathbb{E}_\pi[\sum_{t=0}^{T-1} \gamma^t r_t \mid s_0 = s]$, the action-value function is $Q_\pi(s, a) := \mathbb{E}_\pi[\sum_{t=0}^{T-1} \gamma^t r_t \mid s_0 = s, a_0 = a]$, and the overall policy performance is $J_\pi := \mathbb{E}_{s \sim \mu} V_\pi(s)$.

Policy Evaluation. Policy evaluation refers to estimating $V_\pi(s)$ or its start-state expectation J_π . The simplest approach is Monte Carlo (MC) evaluation, where trajectories are sampled on-policy and averaged as $\hat{J}_\pi^{MC} := \frac{1}{N} \sum_{i=1}^N g(h_i)$. Since on-policy evaluation can be costly, off-policy policy evaluation (OPE) methods estimate policy performance from historical data (Uehara et al., 2022). The standard importance sampling (IS) estimator reweights trajectories from a behavior policy π_b , given by $\hat{J}_\pi^{IS} := \frac{1}{N} \sum_{i=1}^N g(h_i) \prod_{t=0}^{T^i-1} \frac{\pi(a_t^i | s_t^i)}{\pi_b(a_t^i | s_t^i)}$. Per-decision importance sampling (PDIS) (Precup et al., 2000) applies the weights step by step, leading to $\hat{J}_\pi^{PDIS} := \frac{1}{N} \sum_{i=1}^N \sum_{t=0}^{T^i-1} \gamma^t r_t^i \prod_{k=0}^t \frac{\pi(a_k^i | s_k^i)}{\pi_b(a_k^i | s_k^i)}$, which reduces variance compared to trajectory-level IS. Fitted Q-Evaluation (FQE) (Le et al., 2019) instead learns the Q-function of the evaluation policy via Bellman

consistency and derives J_π from the learned value function. Doubly robust (DR) estimators (Jiang & Li, 2016; Thomas & Brunskill, 2016) combine PDIS with approximate value functions \hat{Q} and \hat{V} ; a common formulation is $\hat{J}_\pi^{DR} := \frac{1}{N} \sum_{i=1}^N [\hat{V}(s_0^i) + \sum_{t=0}^{T^i-1} \gamma^t w_t^i (r_t^i + \gamma \hat{V}(s_{t+1}^i) - \hat{Q}(s_t^i, a_t^i))]$, where $w_t^i = \prod_{k=0}^t \frac{\pi(a_k^i | s_k^i)}{\pi_b(a_k^i | s_k^i)}$. DR estimators reduce variance while maintaining consistency if either the importance weights or the value approximations are accurate. For further discussion, we refer to the survey by Uehara et al. (2022). In this work, we compare against FQE, TIS, PDIS, and DR.

In the upcoming section, we first introduce evaluation-aware reinforcement learning (EvA-RL). We then provide a theoretical analysis of this RL framework, followed by a practical optimization procedure for learning policies that achieve both low evaluation error and high performance.

3 EVALUATION-AWARE REINFORCEMENT LEARNING

The dominant approach in reinforcement learning is to learn an arbitrary policy and to consider evaluation only after learning is complete. In this section, we propose an alternative paradigm where evaluation is central to the policy learning process. Our goal is to learn policies that can be evaluated more accurately using a performance estimator, while still achieving high expected return. We refer to this paradigm as **Evaluation-Aware Reinforcement Learning (EvA-RL)**.

Consider a performance estimator \hat{V}_π which predicts policy π 's value for state s as $\hat{V}_\pi(s)$. The mean squared error (MSE): $\mathbb{E}_{s \sim \mu} [(V_\pi(s) - \hat{V}_\pi(s))^2]$ forms the measure for accuracy of \hat{V}_π predictions. With this, we formulate evaluation-aware policy learning using following objective:

$$\max_{\pi} \mathbb{E}_{s \sim \mu} [V_\pi(s) - \beta(V_\pi(s) - \hat{V}_\pi(s))^2] \quad (1)$$

where $\beta > 0$ is a coefficient that trades off between maximizing expected return and minimizing evaluation error. Throughout this paper, we refer to the ability of a policy to achieve low evaluation error with respect to the estimator as its value-predictability, and to β as the *predictability coefficient*.

In EvA-RL, we propose to estimate the policy performance using rollouts gathered in an *assessment environment*, which can be different from deployment environment. For example, it can be a subset of the deployment environment or a related environment such as a simulation, in which value-informative behavior can be observed more easily, cheaply, or safely than in the deployment environment. Conceptually, this setup is similar to evaluating a human's driving ability through a small, curated driver's test. However, driver's test results are reasonably predictive of broader driving performance largely due to the smooth generalization properties of humans. By contrast, an assessment of a learned neural network policy may not reflect its generalization performance in a different deployment setting. Hence, EvA-RL needs to learn a policy that behaves in a manner such that assessment behaviors are predictive of performance in the deployment environment.

Formally, the EvA-RL framework defines a deployment MDP, $\mathcal{M}_D := \{\mathcal{S}_D, \mathcal{A}_D, P_D, R_D, \gamma_D, \mu_D\}$, and an assessment MDP, $\mathcal{M}_A := \{\mathcal{S}_A, \mathcal{A}_A, P_A, R_A, \gamma_A, \mu_A\}$, such that $\mathcal{S}_D \subseteq \mathbb{R}^d$, $\mathcal{S}_A \subseteq \mathbb{R}^d$, and $\mathcal{A}_A = \mathcal{A}_D$ so that policy π defined for \mathcal{M}_D can also be executed in \mathcal{M}_A . We take μ_A to be a Dirac delta distribution with support only over discrete set of states, $\{s^i \mid s^i \in \mathcal{S}_A; i = 1, 2, \dots, k\}$. This allows us to gather k different assessment rollouts starting at a different state in $\{s^i\}_{i=1}^k$. The state-value function of policy π under the deployment MDP \mathcal{M}_D is denoted as V_D^π . A state-value predictor ψ estimates the value of a query state $s \in \mathcal{S}_D$ using $\{h_i\}_{i=1}^k$ as $\hat{V}_D^\pi(s) = \psi(s, \{h_1, h_2, \dots, h_k\})$. Equivalently, this mechanism can be viewed as *behavior-conditioned value prediction*, $\hat{V}_D^\pi(s) = \psi(s \mid \{h_1, h_2, \dots, h_k\})$, where the assessment rollouts $\{h_i\}_{i=1}^k$ serve as an encoding of the policy under evaluation. This approach of conditional value prediction is conceptually similar to universal value functions (Schaul et al., 2015).

$$\text{We can rewrite the EvA-RL objective as: } \max_{\pi} \mathbb{E}_{s \sim \mu_D} [V_D^\pi(s) - \beta(V_D^\pi(s) - \hat{V}_D^\pi(s))^2] \quad (2)$$

With \hat{V}_D^π estimated from assessment rollouts, we use deployment interactions to approximate the target state-value function V_D^π for policy learning. In a policy-gradient setting, for example, Monte Carlo return samples starting from state s serve as target values $V_D^\pi(s)$, as in standard on-policy policy gradient algorithms such as A2C (Konda & Tsitsiklis, 1999) and TRPO (Schulman et al., 2015).

3.1 THEORETICAL INSIGHTS INTO EVA-RL

Now we analyze the EVA-RL framework, focusing on the properties of resultant policies, their expected returns, and their evaluation errors. For our analysis, we consider $(\mathcal{S}_D, \mathcal{A}_D, P_D, R_D, \gamma_D) = (\mathcal{S}_A, \mathcal{A}_A, P_A, R_A, \gamma_A)$ with $|\mathcal{S}_D| = n$. The start distribution μ_A is assumed to have support over first k states of the common state space with equal probability. Further, we consider deterministic transition and reward dynamics. The policy π is also assumed to be deterministic. For simplicity of analysis, consider a linear transformer (Katharopoulos et al., 2020), ψ_{linear} , for value-prediction:

$$\psi_{\text{linear}}(s, \{h^1, h^2, \dots, h^k\}) = \frac{\sum_{i=1}^k \phi(s)^T \phi(s^i) g(h^i)}{\sum_{i=1}^k \phi(s)^T \phi(s^i)}, \quad (3)$$

where $s \in \mathcal{S}_D$, $\phi : \mathcal{S}_D \rightarrow \mathbb{R}^{d'}$ is a state-embedding function with positive inner products and $g(h^i)$ is the discounted return of assessment trajectory h^i . In the deterministic setting, $g(h^i) = V_D^\pi(s^i)$.

Definition 1. The *value prediction error* of a policy π with respect to predictor ψ , denoted as $\zeta_{\pi, \psi}$, is defined as the mean-squared error of its value estimates: $\zeta_{\pi, \psi}^2 := \mathbb{E}_{s \sim \mu_D} \left[(V_D^\pi(s) - \hat{V}_D^\pi(s))^2 \right]$, where, $\zeta_{\pi, \psi} \geq 0$ and $\hat{V}_D^\pi(s) = \psi(s, \{h_i \mid h_i \sim \pi; s^i \in \mathcal{S}_A; \mathcal{M}_A\}_{i=1}^k)$.

For a finite state space, we can write $\zeta_{\pi, \psi}^2 = \sum_{s \in \mathcal{S}_D} \mu_D(s) (V_D^\pi(s) - \hat{V}_D^\pi(s))^2$. We formulate a hard-constrained variant of the EVA-RL optimization objective (Eq. 2) as follows:

$$\max_{\pi} \sum_{s \in \mathcal{S}_D} \mu_D(s) V_D^\pi(s) \quad \text{s.t.} \quad \zeta_{\pi, \psi}^2 \leq \epsilon^2, \quad (4)$$

where $\epsilon \geq 0$ controls the maximum permissible value prediction error. This formulation of EVA-RL allows us to characterize the overall optimization by upper bounding the prediction error. First, we characterize the hard-constrained problem by relaxing the Bellman consistency constraint on state-values and later provide insights into Bellman-consistent EVA-RL.

Lemma 3.1. *Bellman-relaxed, hard-constrained EVA-RL*

$$\max_{V_D^\pi(s) \in \mathbb{R}} \sum_{s \in \mathcal{S}_D} \mu_D(s) V_D^\pi(s) \quad \text{s.t.} \quad \zeta_{\pi, \psi}^2 \leq \epsilon^2 \quad \text{is a convex optimization problem.} \quad (5)$$

Proof. For a detailed proof, see Appendix A.1. Briefly, the optimization problem can be shown to be a quadratically constrained linear program (Boyd & Vandenberghe, 2004) with a positive semi-definite quadratic constraint. \square

Thus, multiple optimal solutions for V_D^π may exist for the Bellman-relaxed problem 5, each corresponding to a distinct policy. These solutions differ from each other by vectors in the null-space of the quadratic constraint. Incorporating Bellman-consistency constraints in the optimization may still admit multiple optimal V_D^π . This is in contrast to standard RL where the optimal value function is unique (Sutton & Barto, 1998). Additionally, the expected return under Bellman-relaxed optimization forms an upper bound on the expected return under Bellman consistency. We provide the exact expression for the upper bound in Appendix A.3.

Importantly, the Bellman-consistent hard-constrained EvA-RL optimization is not necessarily a convex optimization problem due to the possible non-convex relationship between a policy and its value (Dadashi et al., 2019).

In our work, we develop a policy gradient approach to EvA-RL optimization. The soft-constrained formulation in Eq. 2 is especially well-suited for this approach, as deployment values can be efficiently approximated using Monte Carlo samples when calculating policy gradients. To provide direct insights into our practical EvA-RL optimization, we now establish the relationship between the hard- and soft-constrained optimization problems.

Theorem 3.1. *Any solution $V_D^{\pi^* \epsilon}$ to Bellman-relaxed hard-constrained problem 5 is a solution to the Bellman-relaxed soft-constrained optimization problem*

$$\max_{V_D^{\pi}(s) \in \mathbb{R}} \sum_{s \in \mathcal{S}_D} \mu_D(s) V_D^{\pi}(s) - \beta \zeta_{\pi, \psi}^2, \quad (6)$$

for $\beta = 1/(2\epsilon^2) \times \sum_{s \in \mathcal{S}_D} \mu_D(s) V_D^{\pi^* \epsilon}(s)$. Conversely, any solution $V_D^{\pi^* \beta}$ to the above Bellman-relaxed soft-constrained problem 6 is also a solution to Bellman-relaxed hard-constrained problem 5 with $\epsilon = \zeta_{\pi^* \beta, \psi}$.

Proof. Refer to Appendix A.4 for a detailed proof. \square

Corollary 3.1. *The Bellman-relaxed soft EvA-RL leads to multiple optimal solutions for V_D^{π} .*

Proof. Refer to Appendix A.4 for a detailed proof. \square

Furthermore, the expected return of Bellman-relaxed soft EvA-RL can potentially be unbounded, as any solution $V_D^{\pi^* \beta}$ can be summed with a vector from the null-space of the quadratic constraint without affecting the value prediction error. In practice, however, Bellman consistency constraints impose natural limits on the maximum achievable expected return. Analytically determining this maximum expected return remains challenging due to the inherent non-convexity of Bellman-consistent soft EvA-RL. Nevertheless, it is important to note that Bellman-consistent soft EvA-RL still permits multiple distinct value function solutions. We can further state the following:

Proposition 3.1. *Increasing β in the EvA-RL optimization performed using a fixed value predictor (Eq. 2) monotonically decreases the evaluation error and the expected return of the resultant policy.*

Proof. Refer to Appendix A.5 for a detailed proof. \square

This result does not require any linearity assumption on the value-predictors and implies that *using a fixed value-predictor will lead to a trade-off between the expected return and the evaluation accuracy.*

Additionally, we provide a relationship between value prediction error $\zeta_{\pi, \psi}$ and squared error in the performance estimate of the policy J_{π} using the predictor ψ :

Lemma 3.2. *The MSE in expected return of a policy is bounded above by the square of value prediction error, i.e., if $J_{\pi} = \mathbb{E}_{s \sim \mu_D} V_D^{\pi}(s)$ and $\hat{J}_{\pi} = \mathbb{E}_{s \sim \mu_D} \hat{V}_D^{\pi}(s)$, then $(J_{\pi} - \hat{J}_{\pi})^2 \leq \zeta_{\pi, \psi}^2$.*

Proof. Refer to Appendix A.6 for a detailed proof. \square

By the bound-optimization rationale, minimizing the $\zeta_{\pi, \psi}$ will reduce the provable upper bound on the error in estimation of policy performance and thereby indirectly reduce the error in the overall performance estimate.

3.2 PRACTICAL EVA-RL

Theory highlights that with a fixed value predictor, enforcing more accurate evaluation will inherently lower performance. To mitigate this tradeoff, we propose to co-learn the value predictor alongside the policy. Intuitively, this shifts part of the responsibility of value predictability to the predictor itself, thereby enabling less constrained policy optimization.

We introduce a general transformer-based (Vaswani et al., 2017) state-value predictor. The predictor takes as input the assessment start-states along with the corresponding policy returns and maps a query state to its value estimate in the deployment environment. In principle, the predictor can condition value predictions on entire assessment trajectories $\{h_1, h_2, \dots, h_n\}$, but we found in practice that using only start-states and corresponding returns was sufficient. Figure 1 illustrates the EVA-RL value prediction transformer.

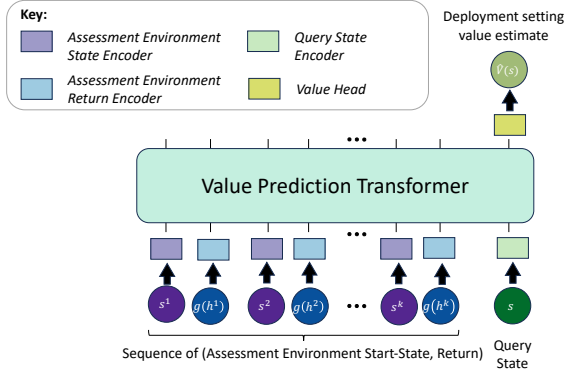


Figure 1: **Value Prediction Transformer:** A transformer encoder that takes as input (i) the start-states of the assessment environment – $\{s^1, s^2, \dots, s^k\}$, (ii) the returns corresponding to the rollouts of policy π starting at these states – $\{g(h_1), g(h_2), \dots, g(h_k)\}$, and (iii) a query state $s \in \mathcal{S}_D$ and outputs an estimate for the value of the query state – $\hat{V}_D^\pi(s)$. The JAX implementation is provided in appendix B.

Let ψ_ϕ and π_θ denote the parametric value predictor and the policy, respectively. Both the policy and the predictor are initialized randomly. Hence, the initial value estimates by ψ_ϕ are arbitrary and cannot be used to provide any meaningful evaluation feedback. To overcome this, we train the policy for a fixed number of updates using a standard on-policy policy gradient algorithm without any evaluation feedback. From policies π_{θ^i} appearing during these updates, we collect assessment returns $\{g(h_A^i) | h_A^i \sim \pi_{\theta^i}; s_A^i; \mathcal{M}_A\}_{i=1}^k$, deployment states $\{s_D^i | s_D^i \sim \mu_D\}_{i=1}^p$ and corresponding returns $\{g(h_D^i) | h_D^i \sim \pi_{\theta^i}; s_D^i; \mathcal{M}_D\}_{i=1}^p$ in a replay buffer \mathcal{B}_ψ . The collected data is then used to train the value predictor, which can then be used to perform evaluation-aware learning. Further, as this learning proceeds, \mathcal{B}_ψ is updated with data from the recent policies such that at any time it contains data from m recent policies. We define the predictor shorthand as $\hat{V}_\phi(s_D; \Xi_A) \triangleq \psi_\phi(s_D, \{s_A^i\}_{i=1}^k, \{g(h_A^i)\}_{i=1}^k)$, where $\Xi_A = \{(s_A^i, g(h_A^i))\}_{i=1}^k$ denotes the assessment dataset. We use the following two-stage update procedure for co-learning predictor along with the policy:

$$\begin{aligned} \phi_{n+1} &\leftarrow \arg \min_{\phi} \mathbb{E}_{(s_D, g(h_D), \Xi_A) \sim \mathcal{B}_\psi} \left[(g(h_D) - \hat{V}_{\phi_n}(s_D; \Xi_A))^2 \right], \\ \theta_{n+1} &\leftarrow \arg \max_{\theta} \mathbb{E}_{s_D \sim \mu_D; h_D \sim \pi_{\theta_n} | s_D, \mathcal{M}_D; \Xi_A \sim \pi_{\theta_n} | \mathcal{M}_A} \left[g(h_D) - \beta (g(h_D) - \hat{V}_{\phi_{n+1}}(s_D; \Xi_A))^2 \right]. \end{aligned}$$

where α_ϕ and α_θ are the learning rates for the predictor and policy, respectively. For both steps, we use gradient-based updates (Eqs. 30 and 31 in appendix).

Characterizing the updates: The value predictor update is essentially a regression of deployment returns, conditioned on the assessment dataset Ξ_A . The policy update step is slightly more nuanced. We will denote the expectation $\mathbb{E}_{s_D \sim \mu_D; h_D \sim \pi_{\theta_n} | s_D, \mathcal{M}_D; \Xi_A \sim \pi_{\theta_n} | \mathcal{M}_A}$ as $\mathbb{E}_{h_D, \Xi_A \sim \pi_{\theta_n}}$. Expanding the policy update gradient

yields:

$$\begin{aligned} \nabla_{\theta} J(\theta) &= \nabla_{\theta} \mathbb{E}_{h_D, \Xi_A \sim \pi_{\theta}} \left[g(h_D) - \beta (g(h_D) - \hat{V}_{\phi}(s_D; \Xi_A))^2 \right] \\ &= \underbrace{\nabla_{\theta} \mathbb{E}_{h_D, \Xi_A \sim \pi_{\theta}} [g(h_D)]}_{\text{standard policy gradient}} - 2\beta \mathbb{E}_{h_D, \Xi_A \sim \pi_{\theta}} \left[(g(h_D) - \hat{V}_{\phi}(s_D; \Xi_A)) (\nabla_{\theta} g(h_D) - \nabla_{\theta} \hat{V}_{\phi}(s_D; \Xi_A)) \right]. \end{aligned} \quad (7)$$

Here, $\nabla_{\theta} g(h_D)$ is the policy gradient computed using the deployment trajectory h_D (Sutton et al., 1999). Further, $\nabla_{\theta} \hat{V}_{\phi}(s_D; \Xi_A)$ denotes the gradient of the predictor’s value estimate with respect to the policy parameters and can be computed via the chain rule: $\nabla_{\theta} \hat{V}_{\phi}(s_D; \Xi_A) = \sum_{i=1}^k \frac{\partial \hat{V}_{\phi}(s_D; \Xi_A)}{\partial g(h_A^i)} \cdot \nabla_{\theta} g(h_A^i)$. This is essentially aggregation of the gradient of the value estimate with respect to each assessment return multiplied by the policy gradient computed using corresponding assessment trajectory.

The two-stage procedure leads to: (i) up-to-date value prediction by the predictor on recent policies, (ii) optimization of the policy performance in the deployment environment, (iii) preferential selection of policies that lead to lower evaluation error, and (iv) inducing assessment behavior that leads to better value predictions via the predictor. The algorithmic pseudo-code for EvA-RL is provided in appendix C.

4 EXPERIMENTS AND RESULTS

In this section, we present experiments designed to answer the following questions: (1) When using a fixed value predictor, does a higher predictability coefficient result in the theoretically suggested impact on returns and evaluation accuracy? And can a co-learned predictor mitigate the tradeoff between these quantities? (2) After learning a policy with EvA-RL, what is the accuracy of a co-learned value predictor compared to standard OPE? (3) How does expected return and evaluation accuracy under the full EvA-RL pipeline compare to the standard RL+OPE pipeline?

Experimental Setup: We evaluate EvA-RL on three discrete-action Gymnax environments (Asterix, Freeway, and Space Invaders) and three continuous-action Brax environments (HalfCheetah, Reacher, and Ant). Our implementation builds on PureJaxRL (Lu et al., 2022). Agents are trained for 10M environment interactions, and results are averaged over 5 random seeds with standard error.

Baselines: We choose the following OPE methods for comparison of state-value estimation: fitted Q-evaluation (FQE), trajectory importance sampling (TIS), per-decision importance sampling (PDIS), and the doubly robust (DR) estimator. For FQE and DR, we adapt code from the Scope-RL library (Kiyohara et al., 2023). We report the mean absolute error (MAE) of the value estimates using ground truth values computed via near-exhaustive on-policy evaluation.

Assessment environment design: We choose the assessment environment to have the same state and action spaces and same transition and reward dynamics as the deployment environment. We choose $\gamma_{ae} = 1$ and select the start states for the assessment environment by sampling 5 states from rollouts of a base RL policy trained using standard A2C. Further, we fix the horizon length for the assessment environment to be 10 steps for discrete action environments and 25 steps for continuous action environments. Example assessment start-states for MinAtar environments are given in appendix E.

Detailed list of hyperparameters used in the experiments is provided in appendix D. The code for the experiments is provided in the supplementary material.

4.1 RESULTS ON DISCRETE-ACTION SPACES

(1) EvA-RL with a fixed value predictor. We first establish that EvA-RL can learn policies with greater value predictability, and that the theoretical tradeoff between predictability and expected return manifests

empirically when using a fixed value predictor. To conduct this experiment, we train a transformer-based predictor on policy data collected from all policies encountered during a standard A2C training run of 10M environment interactions. We then freeze this predictor and perform evaluation-aware policy learning from scratch. We vary the predictability coefficient β and track both the returns and evaluation errors of the resulting policies as a function of β . The results are shown in Figure 2. We observe that the frozen predictor yields decreased evaluation error as β increases. However, this improvement comes at the cost of reduced returns, confirming the tradeoff predicted by Corollary 3.1. Ideally, a perfect value predictor would achieve zero evaluation error and thus yield the same learning dynamics as standard RL ($\beta = 0$). However, developing such a perfect predictor is challenging in practice, and the generalization limitations of pre-training can lead to the observed tradeoff between evaluation accuracy and expected return.

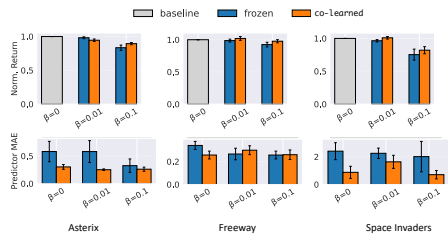


Figure 2: *EvA-RL with a pre-trained value predictor.* Top: normalized returns compared to the standard RL baseline ($\beta = 0$). Bottom: predictor MAE. With a frozen predictor, increasing β decreases MAE but also reduces returns. Co-learning allows for better performance while maintaining low evaluation error.

Additionally, we conduct a variation of this experiment where we allow the value predictor to co-learn alongside the policy at a small learning rate. As shown in Figure 2, this approach enables us to mitigate the return-evaluation error tradeoff by improving policy performance while maintaining low evaluation error.

(2) Comparison of co-learned value predictor with OPE methods. The previous experiment demonstrated the benefits of co-learning the value predictor. We now investigate how well this co-learned predictor performs compared to OPE methods commonly used for policy evaluation. In this experiment, we consider a more challenging setup for EvA-RL in which no prior policy data is available to pre-train the predictor, requiring us to co-learn the value predictor alongside the policy from scratch. As described in Section 3.2, during initial iterations, we train the policy without evaluation feedback and use the collected data to train the value predictor. Once the predictor has sufficiently improved, we perform evaluation-aware policy learning with $\beta \in \{0.01, 0.1\}$. We compare the quality of value estimates from the final co-learned predictor against those from OPE methods. For fairness, we provide all OPE estimators with the same amount of data observed by the predictor during training. Figure 3 shows the comparison of evaluation errors across different performance estimators. We observe that our proposed value predictor consistently achieves much lower evaluation error compared to the OPE estimators. Furthermore, we find that as training progresses, co-learning enables the provision of high-quality value estimates during evaluation-aware learning (refer to the evaluation error learning curves in appendix F).

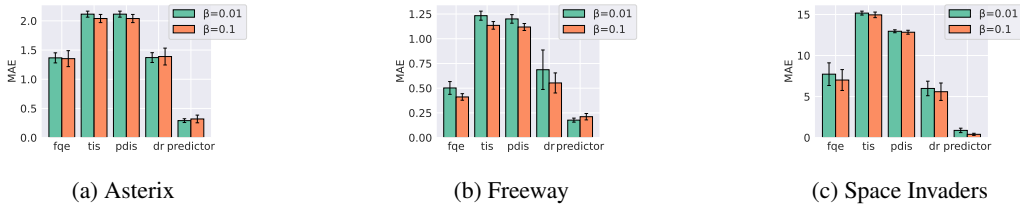


Figure 3: *Co-learned value predictor vs. OPE estimators for EvA-RL policies.* The predictor consistently achieves lower evaluation error showcasing the usefulness of the behavior-conditioned value prediction.

(3) EvA-RL vs. Conventional Learning-then-Evaluation Paradigm. Having established the utility of a co-learned value predictor in EvA-RL, we now compare the overall EvA-RL pipeline with the conventional

RL approach of first learning a policy and then evaluating it (by contrast, note that in the previous experiment both evaluation methods were tested on a policy learned by the EvA-RL learning rule). For this experiment, we train one policy using the standard A2C algorithm and evaluate it with OPE methods. Concurrently, we train another policy using EvA-RL and perform evaluation using the co-learned predictor. The comparison of the resulting expected returns and evaluation errors is shown in Figure 4. We observe that EvA-RL closely matches the performance of standard RL while maintaining substantially lower evaluation error.

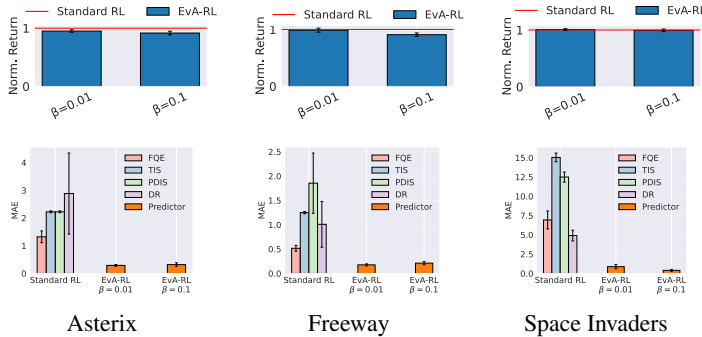


Figure 4: Comparison of standard RL (A2C + OPE) and EvA-RL in discrete-action environments. Top: normalized discounted returns (relative to standard RL; higher is better). Bottom: mean absolute error (MAE) of state-value estimates (lower is better). EvA-RL nearly matches standard RL in its performance while substantially reducing the evaluation error.

4.2 RESULTS ON CONTINUOUS-ACTION SPACES

RL paradigm	HalfCheetah	Reacher	Ant
Standard RL w/ FQE	29.50 ± 9.45	57.28 ± 6.21	49.56 ± 9.77
Standard RL w/ PDIS	3.31 ± 1.61	51.33 ± 37.37	25.91 ± 8.10
Standard RL w/ DR	6.16 ± 2.17	32.33 ± 5.95	10.65 ± 4.51
EvA-RL w/ Predictor	3.46 ± 0.94	13.02 ± 0.65	2.85 ± 0.57

Table 1: EvA-RL often produces more accurate value estimates than OPE estimators in continuous-action environments.

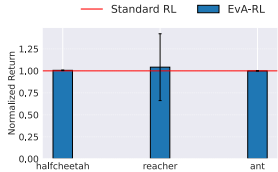


Figure 5: Episodic returns of EvA-RL closely match those of standard RL across continuous-action domains.

We train EvA-RL policies for continuous action tasks of half-cheetah, reacher and ant. In table 1 and figure 5, we showcase results of EvA-RL with $\beta = 5 \times 10^{-4}$. Trajectory-IS estimator (TIS) is excluded as a baseline due to the issue of exponential variance ($T = 1000$). We observe a repetition of the trend observed in the discrete action results – EvA-RL achieves consistent improvement in the evaluation accuracy while maintaining high returns. Learning curves for both discrete and continuous action environments are provided in appendix F.

5 CONCLUSION

Implications of our results for RL development. Our results demonstrate that evaluation-aware learning provides a compelling alternative to the conventional “learning-then-evaluation” paradigm. EvA-RL allows for safer and more efficient RL development by ensuring the policy under update is reliably evaluatable. Moreover, our proposed evaluation using cost-effective assessment environments can serve as an alternative to OPE, and can be used to efficiently evaluate policies in the real-world applications in which testing data is scarce or expensive to collect.

Limitations. Our work depended on randomly sampled states from base policy for defining the assessment start-states. While effective in our experiments, systematic design may lead to stronger behavioral encodings and improved evaluation. In addition, our predictor used only states and returns from the assessment rollouts, rather than full trajectories. Although this design proved sufficient, richer inputs could yield more accurate predictors.

6 ACKNOWLEDGEMENT

This work has taken place in the Safe, Correct, and Aligned Learning and Robotics Lab (SCALAR) at The University of Massachusetts Amherst. SCALAR research is supported in part by the NSF (IIS-2437426), the Long-Term Future Fund, and Open Philanthropy.

REFERENCES

- Marcin Andrychowicz, Bowen Baker, Maciek Chociej, and *et al.* Learning dexterous in-hand manipulation. *The International Journal of Robotics Research*, 2020. First real-world demonstration of vision-based RL on a 24-DoF hand. 1
- Stephen Boyd and Lieven Vandenberghe. *Convex optimization*. Cambridge university press, 2004. 4, 13
- Robert Dadashi, Adrien Ali Taiga, Nicolas Le Roux, Dale Schuurmans, and Marc G Bellemare. The value function polytope in reinforcement learning. In *International Conference on Machine Learning*, pp. 1486–1495. PMLR, 2019. 5
- Isaac Fox, Nilanjan Ray, and K. G. Chase. Deep reinforcement learning for closed-loop glycemic control in type-1 diabetes. *npj Digital Medicine*, 4:64, 2021. 1
- R. Gao, E. Evans, M. Mirhoseini, and D. Riedmiller. Reinforcement learning for data center cooling control. *AI Magazine*, 35(4), 2014. 1
- Nan Jiang and Lihong Li. Doubly robust off-policy value evaluation for reinforcement learning. In *International conference on machine learning*, pp. 652–661. PMLR, 2016. 3
- Dmitry Kalashnikov, Alex Irpan, Peter Pastor, and *et al.* Qt-opt: Scalable deep reinforcement learning for vision-based robotic manipulation. In *Robotics: Science and Systems (RSS)*, 2018. 1
- Angelos Katharopoulos, Apoorv Vyas, Nikolaos Pappas, and François Fleuret. Transformers are rnns: Fast autoregressive transformers with linear attention. In *International conference on machine learning*, pp. 5156–5165. PMLR, 2020. 4
- Haruka Kiyohara, Ren Kishimoto, Kosuke Kawakami, Ken Kobayashi, Kazuhide Nataka, and Yuta Saito. Towards assessing and benchmarking risk-return tradeoff of off-policy evaluation. *arXiv preprint arXiv:2311.18207*, 2023. 7
- Matthieu Komorowski, Leo A. Celi, Omar Badawi, and *et al.* The ai clinician learns optimal treatment strategies for sepsis in intensive care. *Nature Medicine*, 24:1716–1720, 2018. 1
- Vijay Konda and John Tsitsiklis. Actor-critic algorithms. *Advances in neural information processing systems*, 12, 1999. 4
- Hoang M. Le, Cameron Voloshin, and Yisong Yue. Batch policy learning under constraints, 2019. URL <https://arxiv.org/abs/1903.08738>. 2
- Qiang Liu, Lihong Li, Ziyang Tang, and Dengyong Zhou. Breaking the curse of horizon: Infinite-horizon off-policy estimation. *Advances in neural information processing systems*, 31, 2018. 1
- Chris Lu, Jakub Kuba, Alistair Letcher, Luke Metz, Christian Schroeder de Witt, and Jakob Foerster. Discovered policy optimisation. *Advances in Neural Information Processing Systems*, 35:16455–16468, 2022. 7, 19

- Doina Precup, Richard S Sutton, and Satinder Singh. Eligibility traces for off-policy policy evaluation. In *ICML*, volume 2000, pp. 759–766. Citeseer, 2000. 2
- Martin L Puterman. Markov decision processes. *Handbooks in operations research and management science*, 2:331–434, 1990. 2
- Tom Schaul, Daniel Horgan, Karol Gregor, and David Silver. Universal value function approximators. In Francis Bach and David Blei (eds.), *Proceedings of the 32nd International Conference on Machine Learning*, volume 37 of *Proceedings of Machine Learning Research*, pp. 1312–1320, Lille, France, 07–09 Jul 2015. PMLR. URL <https://proceedings.mlr.press/v37/schaul15.html>. 3
- John Schulman, Sergey Levine, Pieter Abbeel, Michael Jordan, and Philipp Moritz. Trust region policy optimization. In *International conference on machine learning*, pp. 1889–1897. PMLR, 2015. 4
- Richard S Sutton and Andrew G Barto. Introduction to reinforcement learning, 1998. 4
- Richard S Sutton, David McAllester, Satinder Singh, and Yishay Mansour. Policy gradient methods for reinforcement learning with function approximation. *Advances in neural information processing systems*, 12, 1999. 7
- Philip Thomas and Emma Brunskill. Data-efficient off-policy policy evaluation for reinforcement learning. In *International conference on machine learning*, pp. 2139–2148. PMLR, 2016. 3
- Philip Thomas, Georgios Theodorou, and Mohammad Ghavamzadeh. High-confidence off-policy evaluation. In *Proceedings of the AAAI Conference on Artificial Intelligence*, volume 29, 2015. 1
- Masatoshi Uehara, Chengchun Shi, and Nathan Kallus. A review of off-policy evaluation in reinforcement learning. *arXiv preprint arXiv:2212.06355*, 2022. 2, 3
- Ashish Vaswani, Noam Shazeer, Niki Parmar, Jakob Uszkoreit, Llion Jones, Aidan N Gomez, Łukasz Kaiser, and Illia Polosukhin. Attention is all you need. *Advances in neural information processing systems*, 30, 2017. 2, 6
- Y. Zheng, J. Wen, and Y. S. Chong. Optimal control of hvac systems using deep reinforcement learning. *Applied Energy*, 295:117116, 2021. 1

A THEOREMS AND PROOFS

This appendix provides a detailed theoretical analysis of the predictability objectives used in EvA-RL, including vectorized formulations, convexity proofs, monotonicity properties, and the relationship between soft and hard constraints.

A.1 VECTORIZED FORMULATION OF EVA-RL OBJECTIVES FOR ANALYSIS

To facilitate theoretical analysis, we first recast the EvA-RL objective in a vectorized form. This approach enables us to leverage linear algebraic tools for understanding the structure and properties of the optimization problem.

Recall the soft EvA-RL objective:

$$\max_{\pi} \mathbb{E}_{s \sim \mu_D} \left[V_D^{\pi}(s) - \beta (V_D^{\pi}(s) - \hat{V}_D^{\pi}(s))^2 \right]. \quad (8)$$

Let $\mu_D = [\mu_D(s_1), \mu_D(s_2), \dots, \mu_D(s_n)]^T$ denote the start-state distribution, and $V_D^\pi = [V_D^\pi(s_1), \dots, V_D^\pi(s_n)]^T$ the vector of state values. Without loss of generality, we assume the first k states correspond to the start-states of the assessment environment \mathcal{S}_A .

We use a pre-trained linear transformer ψ_{linear} (see Eq. 3 in the main text), and define a similarity function $f : \mathcal{S}_D \times \mathcal{S}_D \rightarrow \mathbb{R}^+$ as $f(s, s') = \phi(s)^T \phi(s')$. The transformer can then be written as:

$$\hat{V}_D^\pi(s) = \psi_{\text{linear}}(s, \{h_1, \dots, h_k\}) = \frac{\sum_{s^i \in \mathcal{S}_A} f(s, s^i) g(h^i)}{\sum_{s^i \in \mathcal{S}_A} f(s, s^i)}. \quad (9)$$

To express this in matrix form, we construct a matrix F of dimensions $n \times n$ as follows:

$$F = \begin{bmatrix} f(s^1, s^1) & f(s^1, s^2) & \dots & f(s^1, s^k) & 0 & 0 & \dots & 0 \\ f(s^2, s^1) & f(s^2, s^2) & \dots & f(s^2, s^k) & 0 & 0 & \dots & 0 \\ \vdots & \vdots & \ddots & \vdots & \vdots & \vdots & \ddots & \vdots \\ f(s^k, s^1) & f(s^k, s^2) & \dots & f(s^k, s^k) & 0 & 0 & \dots & 0 \\ f(s_{k+1}, s^1) & f(s_{k+1}, s^2) & \dots & f(s_{k+1}, s^k) & 0 & 0 & \dots & 0 \\ f(s_{k+2}, s^1) & f(s_{k+2}, s^2) & \dots & f(s_{k+2}, s^k) & 0 & 0 & \dots & 0 \\ \vdots & \vdots & \ddots & \vdots & \vdots & \vdots & \ddots & \vdots \\ f(s_n, s^1) & f(s_n, s^2) & \dots & f(s_n, s^k) & 0 & 0 & \dots & 0 \end{bmatrix}_{n \times n} \quad (10)$$

We use superscripted s to denote the start states of the deployment/assessment environment, for the rest of the states, we use subscripted s .

This allows us to write the vector of EvA-RL value estimates as

$$\hat{V}_D^\pi = \text{diag}(F\mathbf{1}_n)^{-1} F V_D^\pi, \quad (11)$$

where $\mathbf{1}_n$ is a vector of ones of size n , and $\text{diag}(F\mathbf{1}_n)$ is a diagonal matrix with $F\mathbf{1}_n$ on its diagonal.

The expected mean-squared error can then be written as

$$\mathbb{E}_{s \sim \mu_D} [V_D^\pi(s) - \hat{V}_D^\pi(s)]^2 = V_D^{\pi T} (I - \text{diag}(F\mathbf{1}_n)^{-1} F)^T \text{diag}(\mu_D) (I - \text{diag}(F\mathbf{1}_n)^{-1} F) V_D^\pi, \quad (12)$$

where $\text{diag}(\mu_D)$ is a diagonal matrix with μ_D on its diagonal.

With this vectorized representation, we can now analyze the properties of the resulting optimization problem, as detailed in the following sections.

We can express the soft EvA-RL objective in equation 8 as:

$$\max_{\pi} \mu_D^T V_D^\pi - \beta [V_D^{\pi T} (I - \text{diag}(F\mathbf{1}_n)^{-1} F)^T \text{diag}(\mu_D) (I - \text{diag}(F\mathbf{1}_n)^{-1} F) V_D^\pi] \quad (13)$$

The hard-constrained EvA-RL objective can be written as:

$$\max_{\pi} \mu_D^T V_D^\pi \quad \text{s.t.} \quad V_D^{\pi T} (I - \text{diag}(F\mathbf{1}_n)^{-1} F)^T \text{diag}(\mu_D) (I - \text{diag}(F\mathbf{1}_n)^{-1} F) V_D^\pi \leq \epsilon^2. \quad (14)$$

A.2 ANALYSIS OF THE OPTIMIZATION PROBLEM

Lemma A.1.

$$\max_{V_D^\pi(s) \in \mathbb{R}} \sum_{s \in \mathcal{S}_D} \mu_D(s) V_D^\pi(s) \quad \text{s.t.} \quad \sum_{s \in \mathcal{S}_D} \mu_D(s) (V_D^\pi(s) - \hat{V}_D^\pi(s))^2 \leq \epsilon^2 \quad \text{is a convex optimization problem.} \quad (15)$$

Proof. As described in the earlier section of the appendix A.1, the vectorized form of given optimization problem can be written as:

$$\max_{V_D^\pi \in \mathbb{R}^n} \mu_D^T V_D^\pi \quad \text{s.t.} \quad V_D^{\pi T} (I - \text{diag}(F1_n)^{-1} F)^T \text{diag}(\mu_D) (I - \text{diag}(F1_n)^{-1} F) V_D^\pi \leq \epsilon^2 \quad (16)$$

In this optimization problem, we have the objective to maximize $\mu_D^T V_D^\pi$, an affine function of V_D^π .

Now we will characterise the predictability constraint. We can observe that this constraint is quadratic in nature. Further, we have $\forall V_D^\pi$,

$$V_D^{\pi T} (I - \text{diag}(F1_n)^{-1} F)^T \text{diag}(\mu_D) (I - \text{diag}(F1_n)^{-1} F) V_D^\pi \geq 0.$$

This means that the matrix $(I - \text{diag}(F1_n)^{-1} F)^T \text{diag}(\mu_D) (I - \text{diag}(F1_n)^{-1} F)$ is a positive semi-definite matrix. As a consequence, the quadratic constraint is also a convex constraint.

Therefore, the problem is an instance of convex quadratic program (QP) over state-values (Boyd & Vandenberghe, 2004). It can further be categorized as a quadratically constrained linear program (QCLP). \square

A.3 UPPER BOUND ON THE EXPECTED RETURN IN BELLMAN-CONSISTENT EVA-RL

The value of the objective function at the solution for a problem of the form:

$$\max_x a^T x \quad \text{s.t.} \quad x^T Q x \leq \epsilon^2 \quad (17)$$

where $a \in \mathbb{R}^n$ and $Q \in \mathbb{R}^{n \times n}$ is a positive semi-definite matrix, is given by:

$$a^T x^* = \epsilon \sqrt{a^T Q^\dagger a} \quad (18)$$

where Q^\dagger is the pseudo-inverse of Q .

We know that the expected return under Bellman consistency is strictly upper bounded by the expected return under Bellman-relaxed optimization. This bound is given by:

$$\epsilon \sqrt{\mu_D^T [(I - \text{diag}(F1_n)^{-1} F)^T \text{diag}(\mu_D) (I - \text{diag}(F1_n)^{-1} F)]^\dagger \mu_D}$$

A.4 RELATIONSHIP BETWEEN SOFT AND HARD CONSTRAINED PREDICTABILITY OPTIMIZATION

Theorem A.1. Any solution $V_D^{\pi_\epsilon^*}$ to Bellman-relaxed hard-constrained problem 5 is a solution to the Bellman-relaxed soft-constrained optimization problem

$$\max_{V_D^\pi(s) \in \mathbb{R}} \sum_{s \in \mathcal{S}_D} \mu_D(s) V_D^\pi(s) - \beta \zeta_{\pi, \psi}^2, \quad (19)$$

for $\beta = 1/(2\epsilon^2) \times \sum_{s \in \mathcal{S}_D} \mu_D(s) V_D^{\pi_\epsilon^*}(s)$. Conversely, any solution $V_D^{\pi_\beta^*}$ to the above Bellman-relaxed soft-constrained problem is also a solution to Bellman-relaxed hard-constrained problem 5 with $\epsilon = \zeta_{\pi_\beta^*, \psi}$.

Proof. We can write the the objective $\max_{V_D^\pi} \sum_{s \in \mathcal{S}_D} \mu_D(s) V_D^\pi(s) - \beta \sum_{s \in \mathcal{S}_D} \mu_D(s) (V_D^\pi(s) - \hat{V}_D^\pi(s))^2$ in a vectorized form as,

$$\max_{V_D^\pi} \mu_D^T V_D^\pi - \beta V_D^{\pi T} (I - \text{diag}(F1_n)^{-1} F)^T \text{diag}(\mu_D) (I - \text{diag}(F1_n)^{-1} F) V_D^\pi \quad (20)$$

Let $(I - \text{diag}(F1_n)^{-1}F)^T \text{diag}(\mu_D)(I - \text{diag}(F1_n)^{-1}F) = Q$. We have Q to be positive semi-definite matrix from earlier proof A.1. Then, the optimization problem can be rewritten as:

$$\max_{V_D^\pi} \mu_D^T V_D^\pi - \beta V_D^{\pi T} Q V_D^\pi \quad (21)$$

This is a quadratic optimization problem with positive semidefinite matrix corresponding to the quadratic term. The solutions of this optimization problem can be characterized by the first-order optimality condition:

$$\nabla_{V_D^\pi} (\mu_D^T V_D^\pi - \beta V_D^{\pi T} Q V_D^\pi) = 0 \implies \mu_D - 2\beta Q V_D^\pi = 0 \implies Q V_D^\pi = \frac{1}{2\beta} \mu_D \quad (22)$$

We have $V_D^{\pi^* \beta}$ as one of the solutions to the above equation implying $Q V_D^{\pi^* \beta} = \frac{1}{2\beta} \mu_D$.

We set

$$\epsilon^2 = \sum_{s \in \mathcal{S}_D} \mu_D(s) (V_D^{\pi^* \beta}(s) - \hat{V}_D^{\pi^* \beta}(s))^2 \quad (23)$$

$$= V_D^{\pi^* \beta T} (I - \text{diag}(F1_n)^{-1}F)^T \text{diag}(\mu_D) (I - \text{diag}(F1_n)^{-1}F) V_D^{\pi^* \beta} \quad (24)$$

To prove that for this ϵ , $V_D^{\pi^* \beta}$ is also a solution to the hard-constrained optimization problem, consider a global optima of hard-constrained optimization problem $V_D^{\pi^* \epsilon}$. If $V_D^{\pi^* \epsilon} \neq V_D^{\pi^* \beta}$, then

$$\mu_D^T V_D^{\pi^* \epsilon} - \beta V_D^{\pi^* \epsilon T} Q V_D^{\pi^* \epsilon} > \mu_D^T V_D^{\pi^* \beta} - \beta V_D^{\pi^* \beta T} Q V_D^{\pi^* \beta}.$$

This implies that $V_D^{\pi^* \beta}$ is not a maximizer of the soft-constrained optimization problem – a contradiction. Hence, $V_D^{\pi^* \beta}$ is also a solution to the hard-constrained optimization problem.

Also, consider Lagrangian of the hard-constrained optimization problem:

$$\mathcal{L}(V_D^\pi, \lambda) = -\mu_D^T V_D^\pi + \lambda (V_D^{\pi T} Q V_D^\pi - \epsilon^2) \quad (25)$$

At the optimum, we have:

$$\nabla_{V_D^\pi} \mathcal{L}(V_D^{\pi^* \beta}, \lambda) = 0 \implies -\mu_D + 2\lambda Q V_D^{\pi^* \beta} = 0 \implies Q V_D^{\pi^* \beta} = \frac{1}{2\lambda} \mu_D \quad (26)$$

Comparing this with $Q V_D^{\pi^* \beta} = \frac{1}{2\beta} \mu_D$, we have $\lambda = \beta$.

Moreover, we have $\epsilon^2 = V_D^{\pi^* \beta T} Q V_D^{\pi^* \beta} = V_D^{\pi^* \beta T} \mu_D / (2\beta)$, which implies $\beta = \mu_D^T V_D^{\pi^* \beta} / (2\epsilon^2)$. \square

Corollary A.1. *The Bellman-relaxed soft EvA-RL leads to multiple optimal solutions for V_D^π .*

Proof. As the proof of above theorem suggests, any $V_D^\pi \in \mathbb{R}^n$ that satisfies $Q V_D^\pi = \frac{1}{2\beta} \mu_D$ is a valid solution to the optimization problem. Since Q is positive semi-definite, the number of V_D^π 's that satisfy the above equation is infinite. \square

A.5 MONOTONICITY OF PREDICTABILITY GAP AND RETURNS IN PREDICTABILITY OPTIMIZATIONS

Lemma A.2. *Let $x^*(\beta) \in \arg \max_x \{f(x) - \beta g(x)\}$ with $\beta \geq 0$. Then $g(x^*(\beta))$ is non-increasing in β ; i.e. for $\beta_2 > \beta_1 \geq 0$, $g(x^*(\beta_2)) \leq g(x^*(\beta_1))$.*

Proof. Set $x_1 = x^*(\beta_1)$, $x_2 = x^*(\beta_2)$ with $\beta_2 > \beta_1$. Optimality gives

$$f(x_1) - \beta_1 g(x_1) \geq f(x_2) - \beta_1 g(x_2), \quad f(x_2) - \beta_2 g(x_2) \geq f(x_1) - \beta_2 g(x_1).$$

If $g(x_2) > g(x_1)$, adding the two inequalities yields $0 \geq (\beta_2 - \beta_1)(g(x_2) - g(x_1)) > 0$, a contradiction; hence $g(x_2) \leq g(x_1)$. \square

Lemma A.3. *Under the same setup, $f(x^*(\beta))$ is non-increasing in β ; explicitly, for $\beta_2 > \beta_1 \geq 0$, $f(x^*(\beta_2)) \leq f(x^*(\beta_1))$.*

Proof. With x_1, x_2 as above, Lemma A.2 gives $g(x_1) \geq g(x_2)$. Optimality at β_1 implies

$$f(x_1) - \beta_1 g(x_1) \geq f(x_2) - \beta_1 g(x_2) \implies f(x_1) - f(x_2) \geq \beta_1 (g(x_1) - g(x_2)) \geq 0.$$

Hence $f(x_2) \leq f(x_1)$. \square

Proposition A.1. *Increasing β in the EvA-RL optimization performed using a fixed value predictor (Eq. 2) monotonically decreases the evaluation error and the expected return of the resultant policy.*

Proof. Consider EvA-RL predictability objective 2 written below:

$$\max_{\pi} \sum_{s \in \mathcal{S}_D} \mu_D(s) V_D^{\pi}(s) - \beta \sum_{s \in \mathcal{S}_D} \mu_D(s) (V_D^{\pi}(s) - \hat{V}_D^{\pi}(s))^2 \quad (27)$$

and its simplified version 6 where we search for real-valued value functions:

$$\max_{V_D^{\pi} \in \mathbb{R}^n} \sum_{s \in \mathcal{S}_D} \mu_D(s) V_D^{\pi}(s) - \beta \sum_{s \in \mathcal{S}_D} \mu_D(s) (V_D^{\pi}(s) - \hat{V}_D^{\pi}(s))^2 \quad (28)$$

Let $0 \leq \beta_1 < \beta_2$. If $V_D^{\pi_{\beta_1}^*}$ and $V_D^{\pi_{\beta_2}^*}$ are optima of the simplified soft predictability objective, we have from lemmas A.2 and A.3, $\mu_D^T V_D^{\pi_{\beta_1}^*} \leq \mu_D^T V_D^{\pi_{\beta_2}^*}$. Also, if $\zeta_{\pi_{\beta_1}^*, \psi}$ and $\zeta_{\pi_{\beta_2}^*, \psi}$ are the evaluation errors corresponding to $V_D^{\pi_{\beta_1}^*}$ and $V_D^{\pi_{\beta_2}^*}$, we have $\zeta_{\pi_{\beta_1}^*, \psi} < \zeta_{\pi_{\beta_2}^*, \psi}$.

When we consider additional Bellman constraints for characterizing the return and the evaluation error of the original soft predictability problem over policies, the monotonicity results on simplified optimization objective straightforwardly extend as lemmas A.2 and A.3 work with any feasible set of x , possibly defined by constraints. \square

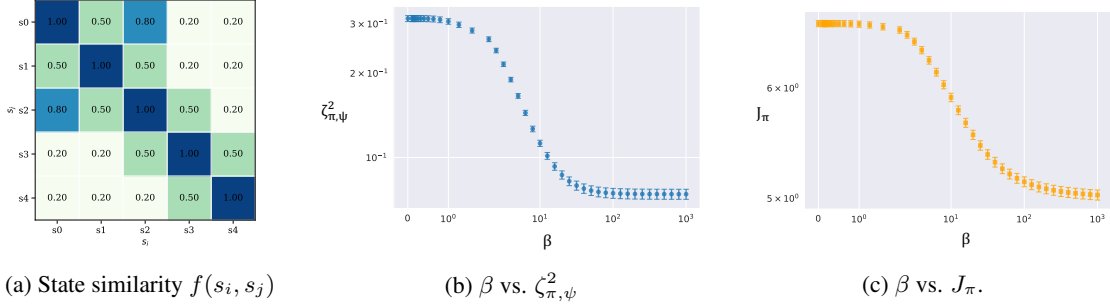


Figure 6: **Effect of predictability coefficient β on the resultant evaluation error, $\zeta_{\pi,\psi}$ and expected return, J_π .** We design a custom MDP with 5 states and 2 actions per state. The state similarity function for this MDP is fixed as shown in sub-figure 6a. States s_0 and s_2 together form the assessment environment. We use uniform distribution over states as our start-state distribution and set the discount factor to 0.9. For each trial, we randomly sample the transition and reward dynamics of this MDP, and solve soft predictability optimization by training a softmax policy for a chosen value of β . In subfigures 6b and 6c, we report the resultant squared evaluation error $\zeta_{\pi,\psi}^2$ and the expected return J_π , respectively. Each data point depicts the average of 1000 random trials along with standard error for each value of β . We can observe that both the gap and the return monotonically decrease as β increases.

A.6 POLICY EVALUATION OF EVA-RL POLICIES

Lemma A.4. *The squared error in estimation of the true performance of the policy: $J_\pi = \mathbb{E}_{s \sim \mu_D} V_D^\pi(s)$ using predictor's value estimates: $\hat{J}_\pi = \mathbb{E}_{s \sim \mu_D} \hat{V}_D^\pi(s)$, is bounded above by the squared-value prediction error: $(J_\pi - \hat{J}_\pi)^2 \leq \zeta_{\pi,\psi}^2$.*

Proof.

$$\begin{aligned}
(J_\pi - \hat{J}_\pi)^2 &= \left(\sum_{s \in \mathcal{S}_D} \mu_D(s) V_D^\pi(s) - \sum_{s \in \mathcal{S}_D} \mu_D(s) \hat{V}_D^\pi(s) \right)^2 = \left(\sum_{s \in \mathcal{S}_D} \mu_D(s) (V_D^\pi(s) - \hat{V}_D^\pi(s)) \right)^2 \\
&= \sum_{s_1, s_2 \in \mathcal{S}_D} \mu_D(s_1) \mu_D(s_2) (V_D^\pi(s_1) - \hat{V}_D^\pi(s_1)) (V_D^\pi(s_2) - \hat{V}_D^\pi(s_2)) \\
&\leq \sum_{s_1, s_2 \in \mathcal{S}_D} \mu_D(s_1) \mu_D(s_2) |V_D^\pi(s_1) - \hat{V}_D^\pi(s_1)| |V_D^\pi(s_2) - \hat{V}_D^\pi(s_2)| \\
&\leq \sum_{s_1, s_2 \in \mathcal{S}_D} \mu_D(s_1) \mu_D(s_2) ((V_D^\pi(s_1) - \hat{V}_D^\pi(s_1))^2 + (V_D^\pi(s_2) - \hat{V}_D^\pi(s_2))^2) / 2 \\
&= \sum_{s \in \mathcal{S}_D} \mu_D(s) (V_D^\pi(s) - \hat{V}_D^\pi(s))^2 = \zeta_{\pi,\psi}^2
\end{aligned} \tag{29}$$

Here for the first inequality we used the Cauchy-Schwarz inequality and for the second we used AM-GM inequality. The above result can also be written as: $J_\pi \in [\hat{J}_\pi - \zeta_{\pi,\psi}, \hat{J}_\pi + \zeta_{\pi,\psi}]$. \square

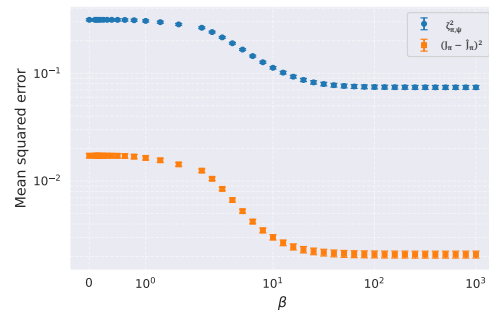


Figure 7: **Policy evaluation using predictor's value estimates.** Here, for the same experimental set-up described in the figure 6, we plot $\zeta_{\pi, \psi}^2$ and $(J_{\pi} - \hat{J}_{\pi})^2$ as β is varied. Each data point represents average over 1000 trials and the error bars denote the standard error. We find that as β increases, the squared error between \hat{J}_{π} w.r.t. J_{π} reduces.

B JAX IMPLEMENTATION OF PREDICTABILITY TRANSFORMER

```

1 import jax.numpy as jnp
2 import flax.linen as nn
3
4 class PredictabilityHead(nn.Module):
5
6     num_heads: int
7     hidden_dim: int
8     num_layers: int
9
10    @nn.compact
11    def __call__(
12        self,
13        assess_env_start_states: jnp.ndarray, # [B,k,obs]
14        assess_env_returns: jnp.ndarray, # [B,k]
15        query_state: jnp.ndarray # [B,obs]
16    ) -> jnp.ndarray: # [B]
17
18        batch_size, k, obs_dim = assess_env_start_states.shape
19        h = self.hidden_dim
20
21        # -----
22        # Token embeddings
23        # -----
24        assess_state_tokens = nn.Dense(h)(assess_env_start_states) # [B,k,h]
25        assess_return_tokens = nn.Dense(h)(assess_env_returns[...], None) # [B,k,h]
26        query_state_token = nn.Dense(h)(query_state[:, None, :]) # [B,1,h]
27
28        # -----
29        # Positional embeddings
30        # -----
31        pos_embeddings = nn.Embed(num_embeddings=k + 1,
32                                features=h)(jnp.arange(k + 1)) # [k + 1,h]
33
34        assess_state_tokens = assess_state_tokens + pos_embeddings[:-1, :] # [B,k,h]
35        assess_return_tokens = assess_return_tokens + pos_embeddings[-1, :] # [B,k,h]
36        query_state_token = query_state_token + pos_embeddings[-1, None, :] # [B,1,h]
37
38        # -----
39        # Full Sequence
40        # -----
41        full_sequence = jnp.concatenate([assess_state_tokens,
42                                        assess_return_tokens, query_state_token], axis=1) # [B,2k+1,h]
43
44        # -----
45        # Transformer
46        # -----
47        x = full_sequence
48        for _ in range(self.num_layers):
49            # Self-attention block
50            y = nn.LayerNorm()(x)
51            y = nn.SelfAttention(num_heads=self.num_heads,
52                               qkv_features=h)(y)
53            x = x + y
54            # Feed-forward block
55            y = nn.LayerNorm()(x)
56            y = nn.relu(nn.Dense(h)(y))
57            y = nn.Dense(h)(y)
58            x = x + y
59
60        query_representation = x[:, -1, :] # last (query) token
61        value_prediction = nn.Dense(1)(query_representation) # [B,1]
62        return jnp.squeeze(value_prediction, -1) # [B]

```

C EVA-RL ALGORITHM

Algorithm 1 Policy optimization with EvA-RL

Require: Assessment start-states $\{s_A^1, \dots, s_A^k\}$, policy π_θ , predictor ψ_ϕ

- 1: Initialize an empty buffer \mathcal{B}_ψ
- 2: **for** $t = 0, 1, 2, \dots$ **do**
- 3: **if** D_ψ has sufficient data **then**
- 4: # PREDICTOR UPDATE
- 5: **for** $i = 1$ to N_{pred} **do**
- 6: Sample a batch from buffer \mathcal{B}_ψ : $(\{s_A^i\}_{i=1}^k, \{g(h_A^i)\}_{i=1}^k, s_D, g(h_D))$.
- 7: Update predictor ϕ via gradient descent

$$\phi_{t+1} = \phi_t - \alpha_\phi \nabla_\phi \left[\mathbb{E}_{(\{s_A^i\}_{i=1}^k, \{g(h_A^i)\}_{i=1}^k, s_D, g(h_D)) \sim D_\psi} (g(h_D) - \psi_{\phi_t}(s_D, \{s_A^i\}_{i=1}^k, \{g(h_A^i)\}_{i=1}^k))^2 \right]_{\phi=\phi_t} \quad (30)$$

- 8: **end for**
- 9: **end if**
- 10: # POLICY UPDATE
- 11: **for** $j = 1$ to N_{policy} **do**
- 12: Collect on-policy rollouts from deployment environment and assessment environment using current policy π_θ .
- 13: **if** Predictor update took place **then**
- 14: Update θ via gradient ascent

$$\theta_{t+1} = \theta_t + \alpha_\theta \nabla_\theta \left[\mathbb{E}_{s_D \sim \mu_D; h_D \sim \pi_\theta | s_D, M_D} (g(h_D) - \beta (g(h_D) - \psi_{\phi_{t+1}}(s_D, \{s_A^i\}_{i=1}^k, \{g(h_A^i)\}_{i=1}^k)))^2 \right]_{\theta=\theta_t} \quad (31)$$

- 15: **else**
 - 16: Update θ via gradient ascent using only the policy gradient (without adding the gradient of predictability loss)
 - 17: **end if**
 - 18: Append assessment rollouts $\{g(h_A^i)\}_{i=1}^k$, deployment states s_D and their returns $g(h_D)$ to buffer \mathcal{B}_ψ
 - 19: **end for**
 - 20: **end for**
-

D HYPERPARAMETER DETAILS

In this section, we provide details of the hyperparameters pertaining to the EvA-RL algorithm. The hyperparameters for policy gradient optimization using advantage-actor critic follow the default values in the PureJaxRL library (Lu et al., 2022).

D.1 DISCRETE ACTION SPACE

Sr. No.	Hyperparameter	Value
1	Number of Environments	64
2	Number of Steps per Environment	100
3	Total Timesteps	1e7
4	Assessment Trajectory Length	10
5	General Trajectory Length	200
6	Learning Rate	1e-4
7	Number of Epochs	100
8	Number of Heads in Transformer	4
9	Number of Layers in Transformer	4
10	Hidden Dimension in Transformer	16
11	Number of Assessment Start States	5
12	Batch Size	256
13	Predictability Coefficient	0, 1e-2, 1e-1
14	Number of Predictor Updates	5
15	Seed	0, 1, 2, 3, 4

D.2 CONTINUOUS ACTION SPACE

Sr. No.	Hyperparameter	Value
1	Number of Environments	2048
2	Number of Steps per Environment	10
3	Total Timesteps	2e7
4	Assessment Trajectory Length	25
5	General Trajectory Length	1000
6	Batch Size	256
7	Learning Rate	1e-4
8	Number of Epochs	100
9	Number of Heads in Transformer	4
10	Number of Layers in Transformer	4
11	Hidden Dimension in Transformer	16
12	Number of Assessment Start States	5
13	Batch Size	256
14	Predictability Coefficient	0, 5e-4
15	Seed	0, 1, 2, 3, 4

E EXAMPLES OF ASSESSMENT ENVIRONMENT STATES

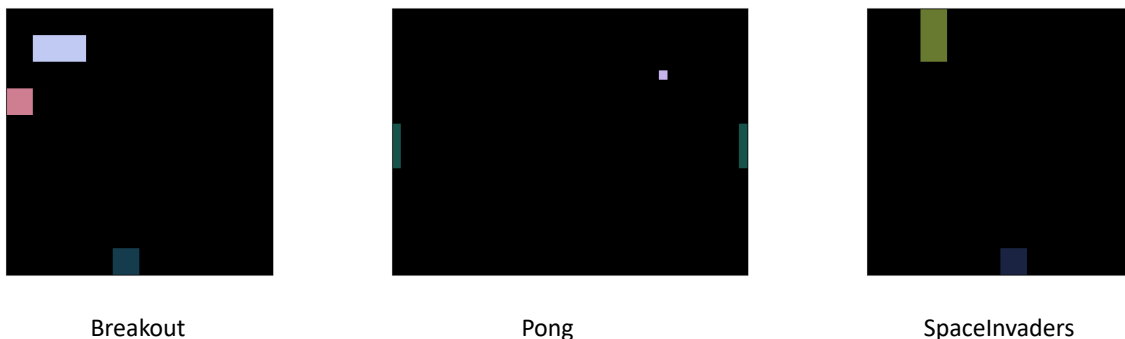


Figure 8: Representative assessment environment start-states for Gymnax environments of Breakout, Pong and SpaceInvaders. In the Breakout environment, we have a ball (in pink) bouncing off the bricks (in white) and the paddle (in grey). In the Pong environment, we have a ball (in white) and two paddles (in grey). In the SpaceInvaders environment, we have an alien spaceship (in green) and the player (in grey). We can use these states to test if the agent can break the bricks in the upper left corner in Breakout, or if the agent can handle ball coming from an edge in Pong, or if the agent can fire at an emancipated alien ship in SpaceInvaders. We will use these behaviors to form a behavioral encoding which we will use to estimate the agent’s performance in true deployment environment.

F ADDITIONAL EXPERIMENTAL RESULTS

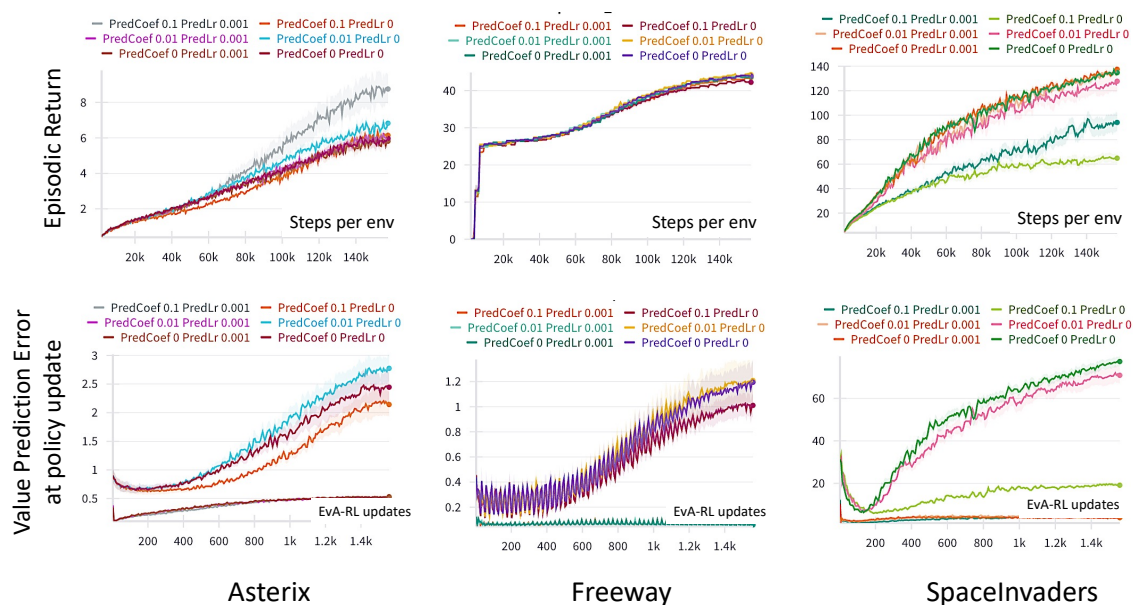


Figure 9: Learning curves for discrete action spaces. The plot shows the episodic return and prediction error computed immediately before updating a policy. We show mean and standard error across 5 different seeds for Asterix, Freeway and SpaceInvaders. The plots show the learning curves for 10 million interactions with the environment. Each plot has predictability coefficient varying among 0, 0.01 and 0.1 and the value predictor learning rate is 0 or $1e-3$. In case of learning rate 0, the predictor is pretrained on data from standard policy gradient RL. Moreover, predictability coefficient 0 corresponds to the standard policy gradient RL. As described in section 4.1, we find that returns of the policies, where the predictor is updated along with the policy closely follow the returns of standard RL policies, while their prediction errors are significantly lower. Increase in predictability coefficient leads to decrease in the return while minimal gains are observed in lowering of the prediction error. Also, when we use a pretrained predictor which is kept frozen during training, the returns are lower than that of simultaneously updated predictor. More importantly, the predictor is being trained on past policies and the error is close to zero when the predictor is co-learned. This allows us to reliably provide evaluation feedback to the policy.

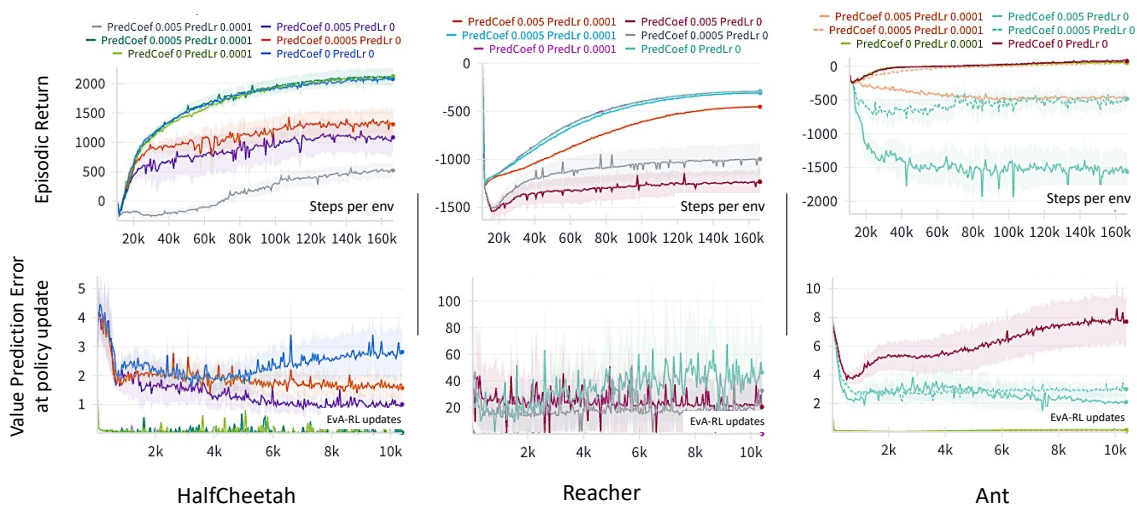


Figure 10: Training curves for continuous action space environments. The plot shows mean and standard error of the episodic return and prediction error computed immediately before updating a policy across 5 different seeds for the Brax environments of halfcheetah, reacher and ant. The plots show the learning curves for 10 million interactions with the environment. Each plot has predictability coefficient varying among 0, 0.0005 and 0.005, and the value predictor learning rate is 0 or $1e-4$. For the case of learning rate to be 0, the predictor is pretrained on data from standard policy gradient RL. The curves here follow similar trends as the discrete action space learning curves described in figure 9. In addition, we find that these environments are more sensitive to changes in the predictability coefficient. The learning rate for the predictor is also lowered compared to the discrete case due to different order of magnitude of the rewards.

G DISCLOSURE ABOUT LLM USAGE

In this work, we used LLMs to develop the code-base for the experiments, check the correctness of the theoretical proofs and to polish the manuscript.